

Microscopic theory of surface-enhanced Raman scattering in noble-metal nanoparticles

Vitaliy N. Pustovit^{1,2} and Tigran V. Shahbazyan¹

¹*Department of Physics and Computational Center for Molecular Structure and Interactions,
Jackson State University, Jackson, MS 39217, USA*

²*Laboratory of Surface Physics, Institute of Surface Chemistry, Kyiv 03164, Ukraine*

We present a microscopic model for surface-enhanced Raman scattering (SERS) from molecules adsorbed on small noble-metal nanoparticles. In the absence of direct overlap of molecular orbitals and electronic states in the metal, the main enhancement source is the strong electric field of the surface plasmon resonance in a nanoparticle acting on a molecule near the surface. In small particles, the electromagnetic enhancement is strongly modified by quantum-size effects. We show that, in nanometer-sized particles, SERS magnitude is determined by a competition between several quantum-size effects such as the Landau damping of surface plasmon resonance and reduced screening near the nanoparticle surface. Using time-dependent local density approximation, we calculate spatial distribution of local fields near the surface and enhancement factor for different nanoparticles sizes.

I. INTRODUCTION

Surface-enhanced Raman scattering (SERS) has been one of the highlights of optical spectroscopy in metal nanostructures during past 25 years.¹ Recent interest in SERS stems from the discovery of extremely strong single-molecule SERS in silver nanoparticle aggregates,^{2,3} as well as from nanoparticle-based applications such as, e.g., biosensors⁴ that rely on sensitivity of SERS to small concentrations of target molecules. The main mechanism of SERS has long been known as electromagnetic (EM) enhancement^{1,5,6,7} of dipole moment of a molecule by the strong local field of surface plasmon (SP) resonance in a nanoparticle. EM mechanism is especially effective when a cluster of nanoparticles is concentrated in a small region ("hot spot").^{8,9,10,11} A combined effect of SP local fields from different particles acting on a molecule trapped in a gap can result in a giant (up to 10^{14}) enhancement of the Raman scattering crosssection.^{12,13,14,15,16,17} Other mechanisms contributing to SERS can involve electron tunneling between a molecule and a nanoparticle.¹⁸

The conventional description of EM enhancement is based on classical Mie scattering theory.^{6,7} The dipole moment of a molecule at distance \mathbf{r}_0 from a particle center is enhanced by a factor $\sim \alpha_p(\omega)/r_0^3$, where $\alpha_p = R^3[(\epsilon - 1)/(\epsilon + 2)]$ is the particle polarizability, R is its radius, and $\epsilon(\omega)$ is metal dielectric function. The far-field of molecular dipole, radiating at Stokes-shifted frequency ω_s , is, in turn, comprised of direct and Mie-scattered fields. The latter contributes another factor $\sim \alpha_p(\omega_s)/r_0^3$, so that the total field enhancement is $\sim \alpha_p(\omega)\alpha_p(\omega_s)/r_0^6$ and Raman crosssection is proportional to $|\alpha_p|^4/r_0^{12}$. At frequencies close to the SP pole in α_p , this enhancement can reach $\sim 10^6$. Note that, within classical description, the dependence of SERS on nanoparticle size, coming from geometrical factor in α , is weak if the molecule is sufficiently close to nanoparticle surface.

The classical approach is valid for relatively large

nanoparticles, where the effect of confining potential on electronic states is negligible. For nanoparticle sizes $R \lesssim 5$ nm, the lifetime of SP is reduced due to the Landau damping by single-particle excitations accompanied by momentum transfer to the surface.¹⁹ This results in a broadening of SP resonance peak by the amount of level spacing at the Fermi energy, $\gamma_s \sim v_F/R$ (v_F is the Fermi velocity), and in the corresponding decrease of the SP field amplitude. For not very small nanoparticles, the effect of Landau damping on SERS can be treated semiclassically¹ by incorporating the quantum-size correction γ_s in the Drude dielectric function of metal. Recent resonance fluorescence measurements on small gold particles,^{20,21,22} however, indicate strong deviations of the plasmon-induced enhancement from that predicted by semiclassical models.⁷ For clusters with electron number $N < 100$, SP lifetime is reduced to several fs and SERS is diminished. Note that some enhancement of Raman signal due to single-particle resonances remains even in small clusters containing several atoms.²³

In this paper, we study SERS for small nanoparticles several nanometers in diameter, i.e., in the intermediate regime between classical particles and small clusters. Our chief observation is that, in this crossover regime, SERS magnitude is determined by interplay between several competing quantum-size effects, including the aforementioned SP Landau damping as well as the modification of electron screening in the surface region. The latter produces an opposite trend towards a *relative increase* of SERS when the molecule is located in a close proximity to the metal surface. The underlying mechanism is related to different effects that the confining potential has on *d*-band and *sp*-band electron states. Namely, the deviation of potential well from the rectangular shape gives rise to a larger *effective* radius for the higher-energy *sp*-electrons.²⁴ This effect is further amplified by the *spillover* of *sp*-band electron density, due to tunneling into the barrier, as contrasted to the essentially step-like density profile of localized *d*-electrons. As a result, in a *surface layer* of thickness $1 - 2$ Å, the

d -electron population is diminished and, hence, the interband (i.e. due to d - sp transitions) polarizability is strongly reduced.^{25,26} The resulting *reduction of screening* in the surface region leads to a greater strength of electron-electron interactions in the sp -band that was observed, e.g., in a faster, as compared to bulk metal, electron relaxation in Ag nanoparticles measured using ultra-fast pump-probe spectroscopy.²⁷ It is, therefore, natural to expect that such underscreening should lead to additional enhancement of local field *outside* of the nanoparticle. Note, however, that here the effect of spillover is twofold: while it leads to an increase of volume fraction of underscreened region and hence to stronger local field, especially in small nanoparticles, it can also, by itself, have an opposite effect by smearing out the otherwise sharp classical boundary.²⁸ Thus, in small nanoparticles, the enhancement magnitude is determined by a delicate interplay of competing quantum-size effects, and must, therefore, be described within a consistent microscopic approach. Such an approach, based on time-dependent local density approximation (TDLDA),²⁹ is developed in this paper.

The paper is organized as follows. In Section II, we derive the general expression for polarizability of molecule-nanoparticle system. In Section III, we derive a self-consistent system for local potential that determines the enhancement factor. In Section IV we present the results of our numerical calculations. Section V concludes the paper.

II. POLARIZABILITY OF MOLECULE-NANOPARTICLE SYSTEM

We start with formulating SERS in terms of quantum transitions in the interacting molecule-nanoparticle system. We assume that the molecule is located at distance r_0 from the nanoparticle center and that the overall system size is much smaller than radiation wavelength so the retardation effects can be ignored.³⁰ In the absence of direct electron tunneling,¹⁸ the interactions within excited molecule-nanoparticle system are caused by *nonradiative transitions* accompanied by energy transfer between a molecule and a nanoparticle, similar to Forster transfer in two-molecule systems.³¹ Namely, an electron-hole pair can nonradiatively recombine by transferring its energy to SP (and vice versa) via dynamically-screened Coulomb interaction.³² Feynman diagrams of processes contributing to polarizability of molecule-nanoparticle system, $\tilde{\alpha}$, are shown in Fig. 1: (a) incident photon with energy ω is absorbed by the molecule and reemitted with Stokes-shifted energy ω_s ; (b) after absorbing a photon, excited molecule nonradiatively recombines transferring its energy to SP in the nanoparticle, which emits a photon; (c) SP, excited by incident light, transfers its energy to the molecule, which emits a photon; and (d) after energy transfer from SP to molecule, the latter transfers the energy back to SP, which emits a photon. Correspondingly,

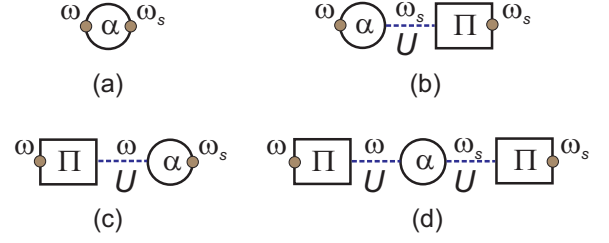


FIG. 1: Nonradiative processes contributing to Raman scattering from a molecule-nanoparticle system.

the system polarizability is (in operator form)

$$\tilde{\alpha} = \alpha + \alpha U \Pi + \Pi U \alpha + \Pi U \alpha U \Pi, \quad (1)$$

where α is molecular polarizability, Π is density-density response function of a nanoparticle in medium, and U is the Coulomb potential. The Raman polarizability is obtained by calculating the matrix element of $\tilde{\alpha}$ between incoming and outgoing photon states with energies ω and ω_s , respectively. The interaction of the molecule with the nanoparticle involves matrix elements $\langle e | \phi(\mathbf{r}) | g \rangle$, where $|g\rangle$ and $|e\rangle$ stand for the molecule ground and excited electronic bands, respectively, and

$$\phi(\omega, \mathbf{r}) = \int d\mathbf{r}_1 d\mathbf{r}_2 U(\mathbf{r} - \mathbf{r}_1) \Pi(\omega, \mathbf{r}_1, \mathbf{r}_2) \phi_0(\mathbf{r}_2) \quad (2)$$

is the nanoparticle response to external photon potential, $\phi_0(\mathbf{r})$. Since the length scale of $\phi(\mathbf{r})$ is much larger than the molecule size, we have $\langle e | \phi(\mathbf{r}) | g \rangle \approx \boldsymbol{\mu} \nabla \phi(\mathbf{r}_0)$, where $\boldsymbol{\mu}$ is the dipole matrix element of corresponding molecular transition.³³ The averaging over random orientations of $\boldsymbol{\mu}$ can be accounted by assuming isotropic Raman polarizability tensor α . The nanoparticle contribution then factors out, $\tilde{\alpha} = \alpha M$, with

$$M = 1 + \frac{1}{E_0^2} \left[\mathbf{E}_0 \cdot \nabla \phi(\omega, \mathbf{r}_0) + \mathbf{E}_0 \cdot \nabla \phi(\omega_s, \mathbf{r}_0) + \nabla \phi(\omega, \mathbf{r}_0) \cdot \nabla \phi(\omega_s, \mathbf{r}_0) \right], \quad (3)$$

where \mathbf{E}_0 is the electric field in the absence of nanoparticle. For incident field, \mathbf{E}_i , polarized along the z -axis, $\phi_0 = -eE_i r \cos \theta$, we have $\mathbf{E}_0 = \mathbf{E}_i / \epsilon_m$, where ϵ_m is the dielectric constant of medium.

III. ENHANCEMENT FACTOR

To evaluate the local potential $\phi(\omega, \mathbf{r})$ within TDLDA approach, we present it in the form

$$\phi(\omega, \mathbf{r}) = e^2 \int d^3 r' \frac{\delta n(\omega, \mathbf{r}')}{|\mathbf{r} - \mathbf{r}'|}, \quad (4)$$

where the induced density,

$$\delta n(\mathbf{r}) = \int d\mathbf{r}' \Pi(\mathbf{r}, \mathbf{r}') \phi_0(\mathbf{r}') = \delta n_s(\mathbf{r}) + \delta n_d(\mathbf{r}) + \delta n_m(\mathbf{r}), \quad (5)$$

contains contributions from *sp*-electrons, *d*-electrons, and surrounding medium, respectively (hereafter we suppress frequency dependence).

We adopt the two-region model that combines a quantum-mechanical description for *sp*-band electrons and phenomenological treatment *d*-electrons with bulk-like ground-state density n_d in the region confined by $R_d < R$.²⁵ This model has been used for calculations of polarizabilities of small Ag nanoparticles and clusters,^{34,35} but it remains reliable for relatively large electron numbers, $N > 1000$. The induced density of *sp*-band electrons is determined from TDLDA equation

$$\delta n_s(\mathbf{r}) = \int d^3r' P_s(\mathbf{r}, \mathbf{r}') [\Phi(\mathbf{r}') + V'_x[n(r')]\delta n_s(\mathbf{r}')], \quad (6)$$

where $\Phi = \phi_0 + \phi$ is the full potential, $P_s(\mathbf{r}, \mathbf{r}')$ is the polarization operator for noninteracting *sp*-electrons, $V'_x[n(r')]$ is the (functional) derivative of the exchange-correlation potential and $n(r)$ is the ground-state electron density. The latter is obtained in a standard way by solving Kohn-Sham equations. To close the system, we need to express the full potential $\Phi(\mathbf{r})$ via $\delta n_s(\mathbf{r})$. This is accomplished by relating $\delta n_d(\mathbf{r})$ and $\delta n_m(\mathbf{r})$ back to $\Phi(\mathbf{r})$ as

$$\begin{aligned} e^2 \delta n_d(\mathbf{r}) &= \nabla [\chi_d(r) \nabla \Phi(\mathbf{r})], \\ e^2 \delta n_m(\mathbf{r}) &= \nabla [\chi_m(r) \nabla \Phi(\mathbf{r})], \end{aligned} \quad (7)$$

where $\chi_d(r) = [(\epsilon_d - 1)/4\pi] \theta(R_d - r)$ is the interband susceptibility with the step function enforcing the boundary conditions and, correspondingly, $\chi_m(r) = [(\epsilon_m - 1)/4\pi] \theta(r - R)$ is the susceptibility of surrounding medium. The derivation is given in Appendix. The final result is conveniently expressed in terms of expansion of $\Phi(\mathbf{r})$ and $\delta n(\mathbf{r})$ in spherical harmonics. For *non-resonant* Raman scattering, only dipole ($L = 1$) terms contribute to the local field. The final expressions for dipole component $\Phi(r)$ can be presented as a decomposition (see the Appendix)

$$\Phi = \frac{1}{\epsilon(r)} [\phi_0(r) + \delta\phi_d(r) + \delta\phi_s(r)], \quad (8)$$

where $\phi_0(r) = -eE_i r$,

$$\begin{aligned} \delta\phi_d(r) &= \beta(r/R) \phi_0(R) \lambda_m (1 - a^3 \lambda_d) / \eta \\ &\quad - \beta(r/R_d) \phi_0(R_d) \lambda_d (1 - 2\lambda_m) / \eta \end{aligned} \quad (9)$$

and

$$\delta\phi_s(r) = \int dr' r'^2 K(r, r') \delta n_s(r'). \quad (10)$$

Here $\epsilon(r) = (\epsilon_d, 1, \epsilon_m)$ for r in the intervals $[(0, R), (R_d, R), (R, \infty)]$, respectively, and

$$\lambda_d = \frac{\epsilon_d - 1}{\epsilon_d + 2}, \quad \lambda_m = \frac{\epsilon_m - 1}{2\epsilon_m + 1}, \quad \eta = 1 - 2a^3 \lambda_d \lambda_m, \quad (11)$$

with $a = R_d/R$. The kernel $K(r, r')$, relating the induced potential and density of *sp*-electrons, is given by

$$\begin{aligned} K(r, r') &= u(r, r') \\ &\quad - \beta(r/R_d) [u(R_d, r') - 2a \lambda_m u(R, r')] \lambda_d / \eta \\ &\quad + \beta(r/R) [u(R, r') - a^2 \lambda_d u(R_d, r')] \lambda_m / \eta, \end{aligned} \quad (12)$$

where $u(r, r') = 4\pi r_{<}/3r_{>}^2$ is the dipole term of Coulomb potential expansion and $\beta(x) = x^{-2}\theta(x-1) - 2x\theta(1-x)$. With decomposition (8), the TDLDA equation (6) takes the form

$$\begin{aligned} \delta n_s(r) &= \int dr' r'^2 P_s(r, r') \frac{1}{\epsilon(r')} [\phi_0(r') + \delta\phi_d(r')] \\ &\quad + \int dr' r'^2 P_s(r, r') \frac{1}{\epsilon(r')} \left[\int dr'' r''^2 K(r', r'') \delta n_s(r'') \right. \\ &\quad \left. + V'_x(r') \delta n_s(r') \right], \end{aligned} \quad (13)$$

Note that $\Phi(r)$ is continuous at $r = R_d, R$.

Equations (8)–(13) determine self-consistently the spatial distribution of local potential near small noble-metal nanoparticles. Here $\delta\phi_d(r)$ is the induced potential due to *d*-electrons and surrounding medium. Their effect on the *sp*-electron potential, $\delta\phi_s(r)$, is encoded in the kernel $K(r, r')$. For $\epsilon_d = \epsilon_m = 1$, we have $K(r, r') = u(r, r')$ and $\delta\phi_d(r) = 0$, recovering the case of simple metal particles in vacuum.

If the molecule is not too close to the surface ($d \gtrsim 1\text{\AA}$), i.e., there is no significant overlap between molecular orbitals and electronic states, then Eqs. (4) and (8)–(13) yield

$$\delta\Phi(r_0) \equiv \frac{1}{\epsilon(r_0)} [\delta\phi_d(r_0) + \delta\phi_s(r_0)] = \frac{eE_i}{\epsilon_m r_0^2} \alpha_p, \quad (14)$$

where $\alpha_p(\omega)$ is the nanoparticle polarizability. The expression for α_p is given in Appendix. Field enhancement coefficient M , Eq. (3), then takes the form

$$\begin{aligned} M &= 1 + (1 + \cos^2 \theta_0) \frac{\alpha_p(\omega) + \alpha_p(\omega_s)}{r_0^3} \\ &\quad + (1 + 3 \cos^2 \theta_0) \frac{\alpha_p(\omega) \alpha_p(\omega_s)}{r_0^6}. \end{aligned} \quad (15)$$

In this case, enhancement retains the same functional dependence on particle polarizability as in classical theory;⁶ however, α_p is now determined microscopically.

IV. NUMERICAL RESULTS AND DISCUSSION

Below we present our results for SERS enhancement factor $|M|^2$ for Ag nanoparticles in a medium with dielectric constant $\epsilon_m = 1.5$. Calculations were carried for number of electrons ranging from $N = 92$ to $N = 3028$,

corresponding to particle diameters in the range $D \approx 1.4 - 4.5$ nm. To ensure spherical symmetry, only closed-shell “magic numbers” were used.³⁶ For such sizes, the Ag band-structure remains intact. The ground state energy spectrum and wave-functions were obtained by solving the Kohn-Sham equations for jellium model²⁹ with the Gunnarsson-Lundqvist exchange-correlation potential;³⁷ the interaction strength was appropriately modified to account for static d -band screening. The ground state density of sp -band electrons, $n(r)$, exhibits characteristic Friedel oscillations, while the spatial extent of spillover is $\simeq 2$ a.u. (see Fig. 2).

These results were used as input in the numerical solution of TDLDA system (8)–(13). The molecule was located along the z -axis ($\theta_0 = 0$) at a distance $d = 5$ a.u. from effective boundary with radius $R = r_s N^{1/3}$, where $r_s = (4\pi n/3)^{-1/3}$ ($r_s = 3.0$ a.u. for Ag), ensuring no direct overlap with the nanoparticle. In the calculation of optical response, the experimental data for $\epsilon_d(\omega)$ in Ag was used³⁸. We also assumed that the Stokes shift is much smaller than $\gamma_s \sim v_F/R$ ($\gamma_s \simeq 0.5$ eV for $D = 3.0$ nm) and ignored the difference between ω and ω_s .

The calculated absorption spectra for different nanoparticle sizes are shown in Fig. 3. For medium dielectric constant $\epsilon_m = 1.5$, the position of SP resonance at $\simeq 3.2$ eV is well below of the interband transition onset at $\simeq 4.0$ eV. As expected, with increasing size the peak width is reduced due to a weaker Landau damping of SP. In order to illustrate the role of interband screening, we also show the results of calculations with $\Delta = 0$. Note that decreasing the surface layer thickness by 1.0 a.u. only somewhat reduces the underscreening; the main effect still comes from the larger spatial extent (about 2 a.u.) of sp -band electron spillover. The effect of underscreened surface region on the absorption is two-fold. The large contrast ratio of ϵ_d in the bulk and surface regions [$\epsilon_d(\omega_{sp}) \approx 5$] leads to a lower, as compared to bulk, *average* value of interband dielectric function in the relevant frequency region. As a result, the peak position for $\Delta = 1.0$ a.u. is slightly blueshifted with respect to that for $\Delta = 0$ ($\delta\omega_{sp} \sim 0.05$ eV). At the same time, for $\Delta = 1.0$ a.u., the peak *amplitude* is larger although the resonance width stays unchanged. The stronger absorption for $\Delta = 1.0$ a.u. is caused by a weaker screening of the SP electric field, that determines the peak oscillator strength, in the surface region.

The calculated local field, E , at resonance frequency is plotted in Fig. 4 vs. molecule-nanoparticle distance, $d = r_0 - R$. The gradual rise of field magnitude on the length scale of electron spillover replaces the discontinuity (for $\epsilon_d, \epsilon_m \neq 1$) of classical field at the sharp boundary. It can be seen that while at $\Delta = 1.0$ a.u. the field amplitude is larger than for $\Delta = 0$, the difference decreases for larger d . Correspondingly, the effect of interband screening on Raman signal enhancement, $|M|^2 \propto |E|^4$, is substantial only when the molecule is located close to the nanoparticle.

In Fig. 5, we plot the enhancement factor $|M|^2$ as a

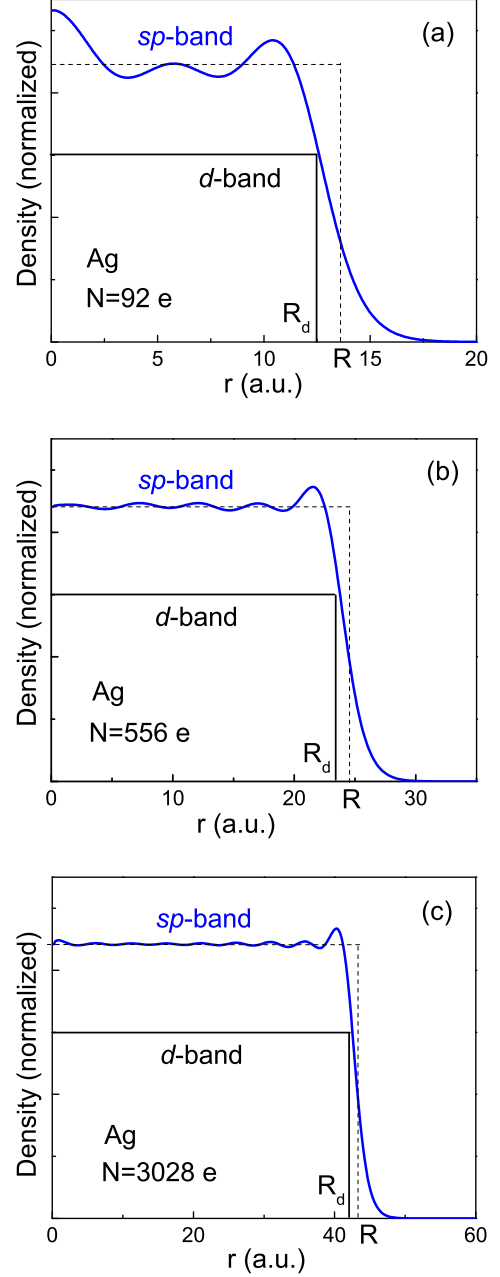


FIG. 2: Calculated ground state density $n(r)$ for Ag nanoparticles is shown for closed-shell electron numbers $N = 92$ (a), $N = 556$ (b), and $N = 3028$ (c).

function of incident light energy for different nanoparticle sizes. Note that the asymmetric shape of the enhancement peak, as compared to the absorption peak, is because the former is determined by the absolute value of polarization, rather than its imaginary part. The general tendency is a decrease of SERS for smaller nanoparticles with the enhancement factor reaching only $|M|^2 \sim 100$ for the smallest nanoparticle size, $D \approx 1.4$ nm. This decrease is mainly related to the Landau damping of SP:

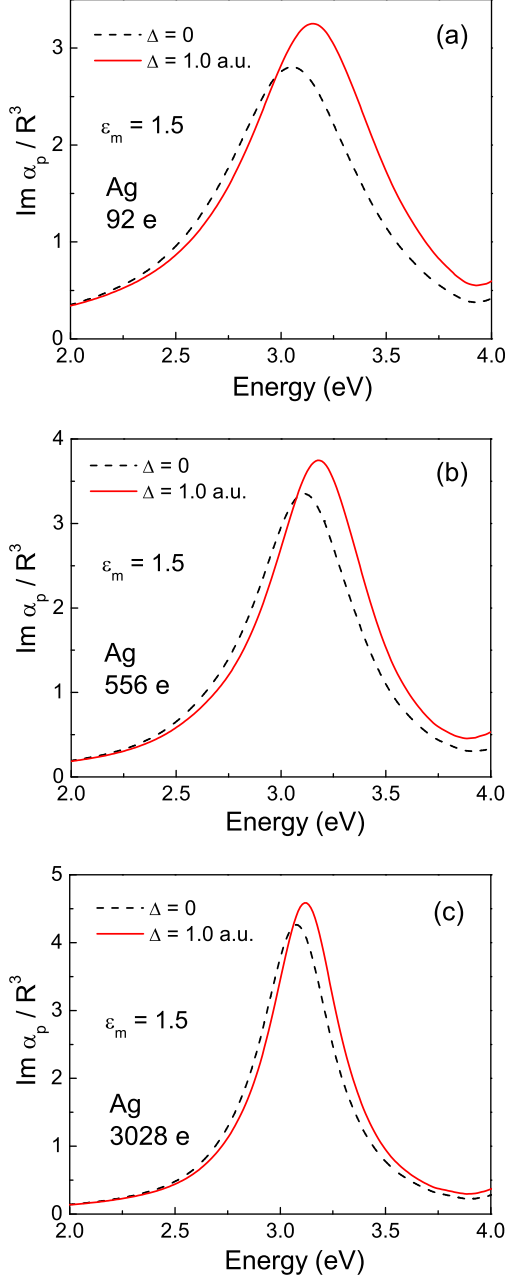


FIG. 3: Calculated absorption spectra for Ag nanoparticles with $\Delta = 0$ (dashed line) and $\Delta = 1.0$ a.u. (solid line) is shown for electron numbers $N = 92$ (a), $N = 556$ (b), and $N = 3028$ (c).

at resonance energy, we have $E \propto 1/\gamma \sim R/v_F$ yielding $|M|^2 \propto R^4$. The comparison of results for $\Delta = 0$ and $\Delta = 1.0$ a.u. shown in Figs. 5(a) and 5(b), respectively, shows that reducing the thickness of surface layer even by 1.0 a.u. substantially affects the enhancement. The role of interband screening is most visible in the dependence of SERS on nanoparticle size plotted in Fig. 6 at resonance frequency for nanoparticle diameters in the

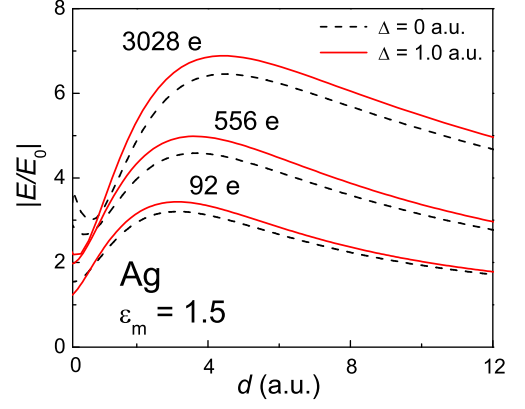


FIG. 4: Calculated local field for several nanoparticles sizes vs. distance from classical boundary for $\Delta = 0$ and $\Delta = 1.0$ a.u.

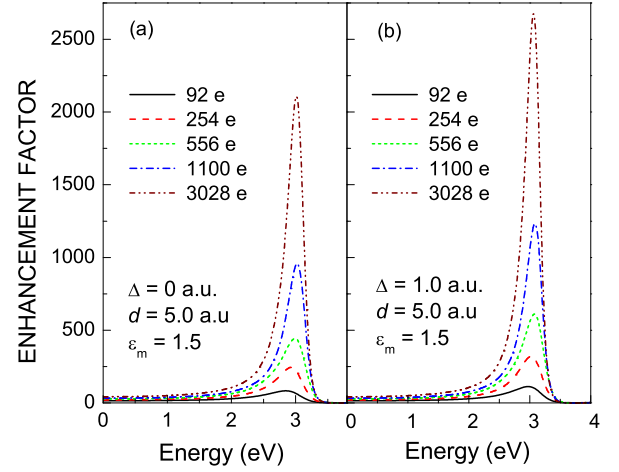


FIG. 5: Calculated enhancement factor $|M|^2$ for different nanoparticle sizes is shown with $\Delta = 0$ (a) and $\Delta = 1.0$ a.u. (b).

range 1.4–4.5 nm. With decreasing size, the enhancement factor drops by an order of magnitude, while overall enhancement is reduced for $\Delta = 0$. Importantly, the latter effect is more pronounced for smaller nanoparticles; for $\Delta = 1.0$ a.u., the enhancement factor is larger by 25% for $N = 3028$ but by 35% for $N = 92$ than for $\Delta = 0$ indicating a more important role of screening in smaller nanoparticles due to larger surface-to-volume ratio. Thus, the proper account of screening gives a *slower* (as compared to semiclassical models) decrease of the enhancement as nanoparticles become smaller. Note, finally, that by keeping Δ constant for different nanoparticle sizes, we somewhat underestimated the screening contribution to SERS; indeed, for smaller nanoparticles, underscreened layer is thicker due to stronger deviations of the confining potential from rectangular shape.

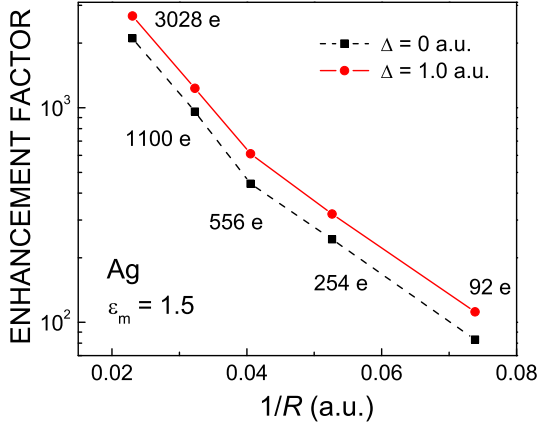


FIG. 6: Calculated enhancement factor $|M|^2$ at resonance frequency vs. nanoparticle size is shown with $\Delta = 0$ and $\Delta = 1.0$ a.u.

V. CONCLUSIONS

We developed a microscopic model for surface-enhanced Raman scattering in noble-metal nanoparticles. Our approach incorporates, in a unified manner, all relevant quantum-size effects that determine the magnitude of Raman signal enhancement for nanometer-sized particles. While the Landau damping of surface plasmons leads to a general decrease of the enhancement for small particles, this trend is partially offset by the reduction of interband screening in the metal boundary region. The additional enhancement of local field is substantial only in a close proximity to the metal surface, and it is more pronounced for smaller nanoparticles where the electron density profile deviates strongly from the classical shape

As a final remark, we considered here a *nonresonant* Raman scattering, i.e. the case when the excitation energy of a molecule is much larger than the SP energy ω_{sp} . In this case, due to small single-molecule polarizability, only linear (in molecule) response needs to be considered and SERS is dominated by a *single* back and forth energy transfer within molecule-nanoparticle system [see Fig. 1(d)]. In the resonant case, *multiple* energy transfer processes give rise to a nonradiative width of the molecular levels and, in general, to a reduction of the enhancement.³⁹ For small molecule-surface separations, these nonradiative processes are dominated by surface-enhanced electron-hole pair generation in the metal. Even in simple metals, these processes are enhanced due to a reduced *intra*band (Thomas-Fermi) screening near the boundary.^{40,41} The issue of nonradiative decay for noble-metal nanoparticles, where *interband* screening effects become important, will be addressed in a future publication.

Acknowledgments

This work was supported by NSF under Grants No. DMR-0305557 and NUE-0407108, by NIH under Grant No. 5 SO6 GM008047-31, and by ARL under Grant No. DAAD19-01-2-0014.

APPENDIX: DERIVATION OF LOCAL POTENTIAL

The full self-consistent potential $\Phi(\mathbf{r}) = \phi(\mathbf{r}) + \phi_0(\mathbf{r})$ satisfies Poisson equation

$$\Phi(\omega, \mathbf{r}) = \phi_0(\mathbf{r}) + e^2 \int d^3r' \frac{\delta n(\omega, \mathbf{r}')}{|\mathbf{r} - \mathbf{r}'|}, \quad (\text{A.1})$$

where the induced density is comprised of *sp*-band, *d*-band and medium contributions, $\delta n(\mathbf{r}) = \delta n_s(\mathbf{r}) + \delta n_d(\mathbf{r}) + \delta n_m(\mathbf{r})$. Using Eq. (7) for δn_m and δn_d and integrating by parts, Eq. (A.1) takes the form

$$\begin{aligned} \epsilon(r)\Phi(\mathbf{r}) = & \phi_0(\mathbf{r}) + e^2 \int d^3r' \frac{\delta n_s(\mathbf{r}')}{|\mathbf{r} - \mathbf{r}'|} \\ & + \frac{\epsilon_d - 1}{4\pi} \int d^3r' \nabla' \cdot \frac{1}{|\mathbf{r} - \mathbf{r}'|} \cdot \nabla' \theta(R_d - r) \Phi(\mathbf{r}') \\ & + \frac{\epsilon_m - 1}{4\pi} \int d^3r' \nabla' \cdot \frac{1}{|\mathbf{r} - \mathbf{r}'|} \cdot \nabla' \theta(r - R) \Phi(\mathbf{r}'), \end{aligned} \quad (\text{A.2})$$

where $\epsilon(r) = (\epsilon_d, 1, \epsilon_m)$ for r in the intervals $[(0, R), (R_d, R), (R, \infty)]$, respectively. Since the source term has the form $\phi_0(\mathbf{r}) = \phi_0(r) \cos \theta = -eE_i r \cos \theta$, we expand Φ and δn_s in terms of spherical harmonics and, keeping only the dipole term ($L = 1$), obtain

$$\begin{aligned} \epsilon(r)\Phi(r) = & \phi_0(r) + e^2 \int dr' r'^2 u(r, r') \delta u_s(r') \\ & - \frac{\epsilon_d - 1}{4\pi} R_d^2 \frac{\partial u(r, R_d)}{\partial R_d} \Phi(R_d) \\ & + \frac{\epsilon_m - 1}{4\pi} R^2 \frac{\partial u(r, R)}{\partial R} \Phi(R), \end{aligned} \quad (\text{A.3})$$

where

$$u(r, r') = \frac{4\pi}{3} \left[\frac{r'}{r^2} \theta(r - r') + \frac{r}{r'^2} \theta(r' - r) \right] \quad (\text{A.4})$$

is the dipole term of the radial component of the Coulomb potential. The above equation can be simplified to

$$\begin{aligned} \epsilon(r)\Phi(r) = & \bar{\phi}(r) - \frac{\epsilon_d - 1}{3} \beta(r/R_d) \Phi(R_d) \\ & + \frac{\epsilon_m - 1}{3} \beta(r/R) \Phi(R), \end{aligned} \quad (\text{A.5})$$

where $\beta(r/R) = (3R^2/4\pi) [\partial u(r, R)/\partial R]$ is given by

$$\beta(x) = x^{-2} \theta(x - 1) - 2x\theta(1 - x), \quad (\text{A.6})$$

and we introduced a shorthand notation

$$\bar{\phi}(r) = \phi_0(r) + e^2 \int dr' r'^2 u(r, r') \delta n_s(r'). \quad (\text{A.7})$$

The boundary values of Φ can be obtained by matching $\Phi(r)$ at $r = R_d, R$, yielding

$$\begin{aligned} (\epsilon_d + 2)\Phi(R_d) + 2a(\epsilon_m - 1)\Phi(R) &= 3\bar{\phi}(R_d), \\ (\epsilon_d - 1)a^2\Phi(R_d) + (2\epsilon_m + 1)\Phi(R) &= 3\bar{\phi}(R), \end{aligned} \quad (\text{A.8})$$

where $a = R_d/R$. Substituting $\Phi(R_d)$ and $\Phi(R)$ back into Eq. (A.5), we arrive at

$$\begin{aligned} \epsilon(r)\Phi(r) &= \bar{\phi}(r) - \beta(r/R_d) \frac{\lambda_d}{\eta} [\bar{\phi}(R_d) - 2a\lambda_m\bar{\phi}(R)] \\ &\quad + \beta(r/R) \frac{\lambda_m}{\eta} [\bar{\phi}(R) - a^2\lambda_d\bar{\phi}(R_d)], \end{aligned} \quad (\text{A.9})$$

where the coefficients λ are given by Eq. (11). Separating out δn_s -dependent contribution, we arrive at Eq. (8).

The expression for nanoparticle polarizability, $\alpha_p(\omega)$, can be obtained from the large- r asymptotics of induced potential, Eq. (14). From Eqs. (9)–(12), we find for

$r \gg R$

$$\delta\phi_d(r) = \frac{eE_i}{r^2} \alpha_d, \quad \delta\phi_s(r) = \frac{eE_i}{r^2} \alpha_s, \quad (\text{A.10})$$

with

$$\begin{aligned} \alpha_d &= R^3 \frac{(1 - \lambda_m)a^3\lambda_d - \lambda_m}{1 - 2a^3\lambda_d\lambda_m}, \\ \alpha_s &= \frac{4\pi}{3eE_i} \left[\int_0^\infty dr' r'^3 \delta n_s(r') \right. \\ &\quad - \frac{\lambda_d - \lambda_m + \lambda_d(1 - 2a^3)}{1 - 2a^3\lambda_d\lambda_m} \int_0^R dr' r'^3 \delta n_s(r') \\ &\quad - \frac{(1 - \lambda_m)a^3\lambda_d - \lambda_m}{1 - 2a^3\lambda_d\lambda_m} R^3 \int_R^\infty dr' \delta n_s(r') \\ &\quad \left. + \frac{(1 + \lambda_m)\lambda_d}{1 - 2a^3\lambda_d\lambda_m} \int_{R_d}^R dr' (r'^3 - R_d^3) \delta n_s(r') \right]. \end{aligned} \quad (\text{A.11})$$

The nanoparticle polarizability is $\alpha_p = \alpha_d + \alpha_s$. Note that for frequencies below interband absorption onset, the d -band/medium contribution α_d is real.

-
- ¹ For a recent review see G. S. Schatz and R. P. Van Duyne, in *Handbook of Vibrational Spectroscopy*, edited by J. M. Chalmers and P. R. Griffiths (Wiley, 2002) p. 1.
- ² S. Nie and S. R. Emory, *Science* **275**, 1102 (1997).
- ³ K. Kneipp, Y. Wang, H. Kneipp, L. T. Perelman, I. Itzkan, R. R. Dasari, and M. S. Feld, *Phys. Rev. Lett.* **78**, 1667 (1997).
- ⁴ Y. C. Cao, R. Jin, and C. A. Mirkin, *Science* **297**, 1536 (2002).
- ⁵ M. Moskovits, *Rev. Mod. Phys.* **57**, 783 (1985).
- ⁶ M. Kerker, D.-S. Wang, and H. Chew, *Appl. Optics* **19**, 4159 (1980).
- ⁷ J. Gersten and A. Nitzan, *J. Chem. Phys.* **75**, 1139 (1981).
- ⁸ K. Kneipp, H. Kneipp, I. Itzkan, R. R. Dasari, and M. S. Feld, *Chem. Rev.* **99**, 2957 (1999), and references therein.
- ⁹ A. M. Michaels, J. Jiang, and L. E. Brus, *J. Phys. Chem. B* **104**, 11965 (2000).
- ¹⁰ M. Moskovits, L. Tay, J. Yang, T. Haslett, *Top. Appl. Phys.* **82**, 215 (2002).
- ¹¹ Z. Wang, S. Pan, T. D. Krauss, H. Du, and L. J. Rothberg, *Proc. Nat. Acad. Sci.* **100**, 8639 (2004).
- ¹² M. I. Stockman, L. N. Pandey, and T. F. George, *Phys. Rev. B* **53**, 2183 (1996).
- ¹³ V. A. Markel, V. M. Shalaev, E. B. Stechel, W. Kim, and R. L. Armstrong, *Phys. Rev. B* **53**, 2425 (1996).
- ¹⁴ H. Xu, E. J. Bjerneld, M. Käll, and L. Börjesson, *Phys. Rev. Lett.* **83**, 4357 (1999).
- ¹⁵ H. Xu, J. Aizpurua, M. Käll, and P. Apell, *Phys. Rev. E* **62**, 4318 (2000).
- ¹⁶ S. Corni and J. Tomasi, *J. Chem. Phys.* **116**, 1156 (2002).
- ¹⁷ K. Li, M. I. Stockman, D. J. Bergman, *Phys. Rev. Lett.* **91**, 227402 (2003).
- ¹⁸ Processes related to charge transfer (chemical mechanism) are out of scope of this paper, see A. Otto, I. Mrozek, H. Grabhorn, and W. J. Akermann, *J. Phys. Cond. Matter* **4**, 1143 (1992).
- ¹⁹ A. Kawabata and R. Kubo, *J. Phys. Soc. Jap.* **21**, 1765 (1966).
- ²⁰ E. Dulkeith, A. C. Morteani, T. Niedereichholz, T. A. Klar, J. Feldmann, S. A. Levi, F. C. J. M. van Veggel, D. N. Reinhoudt, M. Moller, and D. I. Gittins, *Phys. Rev. Lett.* **89**, 203002 (2002).
- ²¹ E. Dulkeith, M. Ringler, T. A. Klar, J. Feldmann, A. M. Javier and W. J. Parak, *Nano Letters* **5**, 585 (2005).
- ²² D. J. Maxwell, J. R. Taylor, and S. Nie, *J. Am. Chem. Soc.* **124**, 9606, (2002).
- ²³ L. Peyser-Capadona, J. Zheng, J. I. Gonzalez, T.-H. Lee, S. A. Patel, and R. M. Dickson, *Phys. Rev. Lett.* **94**, 058301 (2005).
- ²⁴ B. N. J. Persson and E. Zaremba, *Phys. Rev. B* **31**, 1863 (1985).
- ²⁵ A. Liebsch, *Phys. Rev. B* **48**, 11317 (1993); A. Liebsch and W. L. Schaich, *Phys. Rev. B* **52**, 14219 (1995).
- ²⁶ A. Liebsch and W. L. Schaich, *Phys. Rev.* **52**, 14219 (1995).
- ²⁷ C. Voisin D. Christofilos, N. Del Fatti, F. Vallée, B. Prével, E. Cottancin, J. Lermé, M. Pellarin, and M. Broyer, *Phys. Rev. Lett.* **85**, 2200 (2000).
- ²⁸ M. Xu and M. J. Dignam, *J. Chem. Phys.* **96**, 8000 (1992).
- ²⁹ W. Ekardt, *Phys. Rev. B* **31**, 6360 (1985).
- ³⁰ See, e.g., U. Kreibig and M. Vollmer, *Optical Properties of Metal Clusters* (Springer, 1995).
- ³¹ J. R. Lakowicz, *Principles of Fluorescence Spectroscopy* (Plenum, 1999).
- ³² T. V. Shahbazyan, I. E. Perakis, and J.-Y. Bigot, *Phys. Rev. Lett.* **81**, 3120 (1998).
- ³³ See, e.g., D. A. Long, *The Raman Effect* (Wiley, 2002).
- ³⁴ V. V. Kresin, *Phys. Rev.* **51**, 1844 (1995).

- ³⁵ J. Lerme, B. Palpant, B. Prvel, M. Pellarin, M. Treilleux, J. L. Vialle, A. Perez, and M. Broyer, Phys. Rev. Lett. **80**, 5105, (1998).
- ³⁶ E. Koch and O. Gunnarsson, Phys. Rev. B **54**, 5168, (1996)
- ³⁷ O. Gunnarsson and B. Lundqvist, Phys. Rev. B **13**, 4274 (1976).
- ³⁸ *Handbook of Optical Constants of Solids*, Ed. E. D. Palik (Academic Press, 1985).
- ³⁹ H. Xu, X.-H. Wang, M. P. Persson, H. Q. Xu, M. Kall, and P. Johansson Phys. Rev. Lett. **93**, 243002 (2004).
- ⁴⁰ B. N. J. Persson, N. D. Lang, Phys. Rev. B **26**, 5409 (1982).
- ⁴¹ I. A. Larkin, M. I. Stockman, M. Achermann, and V. I. Klimov, Phys. Rev. B. **69**, 121403 (2004).